


# Significance of prediction of the dorsal landmark using three-dimensional computed tomography during laparoscopic lymph node dissection along the proximal splenic artery in gastric cancer

SAGE Open Medicine  
Volume 8: 1–6  
© The Author(s) 2020  
Article reuse guidelines:  
sagepub.com/journals-permissions  
DOI: 10.1177/2050312120936918  
journals.sagepub.com/home/smo



Taro Ikeda<sup>1</sup> , Shingo Kanaji<sup>1</sup>, Gosuke Takiguchi<sup>1</sup>, Naoki Urakawa<sup>1</sup>, Hiroshi Hasegawa<sup>1</sup>, Masashi Yamamoto<sup>1</sup>, Yoshiko Matsuda<sup>1</sup>, Kimihiro Yamashita<sup>1</sup>, Takeru Matsuda<sup>2</sup>, Taro Oshikiri<sup>1</sup>, Tetsu Nakamura<sup>1</sup>, Satoshi Suzuki<sup>1</sup> and Yoshihiro Kakeji<sup>1</sup>

## Abstract

**Objectives:** Dissection of the No. 11p lymph nodes is technically challenging because of variations in anatomical landmarks. This study aimed to determine the accuracy and efficacy of predicting the dorsal landmark of No. 11p lymph node using three-dimensional computed tomography simulation.

**Methods:** Laparoscopic gastrectomy with No. 11p lymph node dissection with preoperative simulation using three-dimensional computed tomography was performed in 24 patients at our institution from October 2016 to May 2018. Initially, preoperative three-dimensional computed tomography findings with operative videos in these 24 patients were compared. The dorsal landmark was defined as an anatomical structure behind the splenic artery on preoperative three-dimensional computed tomography and operative videos. The dorsal landmark of No. 11p lymph node was divided into four types: (1) splenic vein type, (2) splenic vein and pancreas type, (3) pancreas type, and (4) unclear type. Then, to investigate the efficacy of three-dimensional computed tomography, we compared the clinical and pathological features and surgical outcomes of nine patients who underwent preoperative three-dimensional computed tomography simulation (three-dimensional computed tomography group) and 23 patients who did not undergo three-dimensional computed tomography simulation from August 2014 to September 2016 (non-three-dimensional computed tomography group). All procedures were performed by one surgeon certified by the Endoscopic Surgical Skill Qualification System in Japan.

**Results:** The concordance rate between three-dimensional computed tomography and operative videos of the dorsal landmark using three-dimensional computed tomography was 79% (19/24). The operative time of No. 11p lymph node dissection was significantly shorter in the three-dimensional computed tomography group than in the non-three-dimensional computed tomography group (7.7 versus 15.8 min,  $P=0.044$ ).

**Conclusion:** The accuracy of predicting the dorsal landmark of No. 11p lymph node using three-dimensional computed tomography was extremely high. Preoperative simulation with three-dimensional computed tomography was useful in shortening the operative time of No. 11p lymph node dissection.

## Keywords

Gastric cancer, three-dimensional computed tomography, preoperative simulation, lymph nodes along the proximal splenic artery

Date received: 22 August 2019; accepted: 29 May 2020

<sup>1</sup>Division of Gastrointestinal Surgery, Department of Surgery, Graduate School of Medicine, Kobe University, Kobe, Japan

<sup>2</sup>Division of Minimally Invasive Surgery, Department of Surgery, Graduate School of Medicine, Kobe University, Kobe, Japan

## Corresponding author:

Taro Ikeda, Division of Gastrointestinal Surgery, Department of Surgery, Kobe University Graduate School of Medicine, 7-5-2 Kusunoki-chou, Chuo-ku, Kobe 650-0017, Japan.  
Email: tikedata@med.kobe-u.ac.jp



## Introduction

Laparoscopic distal gastrectomy (LDG) for early gastric cancer is widely performed, and several studies have demonstrated its safety and feasibility for early gastric cancer.<sup>1–3</sup> However, LDG for advanced gastric cancer or laparoscopic total gastrectomy (LTG) is not widespread. One reason for this is that dissection of the lymph nodes (LNs) along the proximal splenic artery (No. 11p LNs) is required in LDG with D2 LN dissection and LTG with more than D1 + LN dissection.<sup>4</sup> Inaki et al.<sup>5</sup> reported that the rate of pancreatic fistula for LDG with D2 LN dissection was 3.5%, which is higher than that for D1 + LN dissection. There is a concern that No. 11p LN is located deeply behind the splenic artery at the suprapancreas and that morbidity might increase with dissection. Although the dorsal margin of No. 11p LN is not clearly defined, most surgeons recognize the splenic vein or pancreas behind the splenic artery as a dorsal landmark of No. 11p LN.<sup>6,7</sup> However, although No. 11p LN dissection had sufficient depth, sometimes surgeons encounter cases in which dorsal anatomical structures cannot be detected. Furthermore, it was difficult to identify the organ positional relationship during laparoscopic surgery and it was necessary to simulate the actual laparoscopic view before operation. However, it was difficult to predict the dorsal landmark of No. 11p LN using conventional enhanced computed tomography (CT). This is because conventional two-dimensional (2D)-CT images cannot be rotated and we could not simulate the organ positional relationship in the actual view, including that of the dorsal landmark of No. 11p LN dissection using 2D-CT.<sup>8,9</sup>

Recently, three-dimensional (3D)-CT has been used for preoperative simulation in numerous surgeries. Several studies on gastric surgery have demonstrated the usefulness of prediction for splenic hilum or perigastric vessels.<sup>8–10</sup> However, there is no study on the prediction of anatomical landmarks during LN dissection in gastric surgery using preoperative 3D-CT. Moreover, it is still unclear whether 3D-CT improves surgical outcomes in laparoscopic gastrectomy with No. 11p LN dissection. Thus, this study aimed to clarify the accuracy and efficacy of preoperative 3D-CT simulation for the dorsal landmark of No. 11p LN.

## Materials and methods

All procedures performed in studies involving human participants were in accordance with the ethical standards of the Institutional Review Board of Kobe University Hospital [170119] and the 1964 Declaration of Helsinki and its later amendments or comparable ethical standards. All patients provided written informed consent regarding the use of their data. Preoperative 3D-CT simulation was performed in all patients with advanced gastric cancer who were recommended to undergo LDG with D2 dissection or LTG with D1+ or D2 dissection, which required No. 11p LN dissection from October 2016. We have not performed preoperative 3D-CT simulation before October 2016. Initially, to determine the

accuracy of preoperative 3D-CT, we retrospectively collected data on 3D-CT and video recordings of 24 patients who underwent LDG for advanced gastric cancer or LTG with No. 11p LN dissection with preoperative simulation using 3D-CT at Kobe University Hospital from October 2016 to May 2018. Patients who converted to laparotomy during the surgery or those who could not undergo enhanced CT because of chronic renal failure were excluded. Then, to investigate the efficacy of 3D-CT, we compared the clinical and pathological features and surgical outcomes of nine patients who underwent 3D-CT simulation (3D-CT group) and 23 patients who did not undergo 3D-CT simulation (non-3D-CT group) from August 2014 to September 2016. To exclude the learning curve effect, all procedures in these 32 patients were performed by one surgeon (S.K.) certified by the Endoscopic Surgical Skill Qualification System in Japan.

Preoperative CT scanning was performed using a dual-energy CT scanner (2 × 192 slices, SOMATOM Force, Siemens Healthcare, Erlangen, Germany). The 3D images of arteries, veins, and pancreas were created using ZioStation version 2 (Ziosoft, Tokyo, Japan).

Two surgeons (T.I. and S.K.) determined the preoperative 3D-CT and intraoperative findings from the same images and video recordings. A preoperative 3D-CT image was examined by the caudal view rotated 90° from the front view of 3D-CT, which was the same as the actual intraoperative view during dissection of No. 11p LN during laparoscopic gastrectomy (Figure 1). We defined the scene of No. 11p LN dissection among the scene between the cutting of the left gastric artery to dissection at the middle of the splenic artery and measured the time of the scene as the No. 11p LN dissection time. In the dissection of No. 11p + 11d LNs, we measured half of the dissection time from the cutting of the left gastric artery to dissection at the end of the splenic artery. In the case of LTG with D2 dissection, the No. 11p LN part was defined as the scene until the middle of the splenic artery in the same method. In this study, we divided the 3D-CT and operative findings of the dorsal landmark of No. 11p LN into four types: (1) splenic vein (SV) type, (2) splenic vein and pancreas (SV + P) type, (3) pancreas (P) type, and (4) unclear type. We defined the dorsal landmark of No. 11p LN as an anatomical structure well exposed behind the splenic artery on the video recording.

In gastric cancer staging, we used the International Union Against Cancer TNM staging system<sup>11</sup> and defined the LN stations based on the Japanese Gastric Cancer Association definitions.<sup>12</sup> We determined postoperative morbidity using the Clavien–Dindo classification.<sup>13</sup>

## Statistical analysis

Statistical analysis was performed using JMP version 11.2.0 software (SAS Institute, Inc., Cary, NC, USA). Continuous variables are presented as medians (range). Statistical tests were performed using Fisher's exact test and Mann–Whitney *U* test. A *P* value of <0.05 was considered statistically significant.

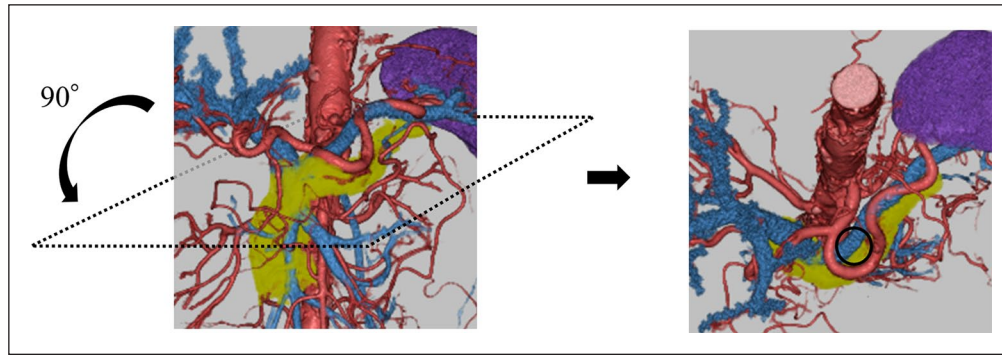


**Figure 1.** We considered the round area (○) as the dorsal landmark of No. 11p LN with a caudal view rotated 90° from the front view of 3D-CT.

**Table 1.** Dorsal landmark of No. 11p LNs in preoperative 3D-CT and operative videos.

| Dorsal landmark of No. 11p LN | Findings in 3D-CT (n=24) | Findings in operative videos | Concordance rate between 3D-CT and operative videos |
|-------------------------------|--------------------------|------------------------------|---|
| SV                            | 12 (50%)                 | 12                           | 100%  |
| SV + P                        | 7 (29%)                  | 4                            | 57%   |
| P                             | 1 (4%)                   | 0                            | 0%  |
| Unclear                       | 4 (17%)                  | 3                            | 75%   |
| Total                         |                          |                              | 79%   |

LNs: lymph nodes; 3D-CT: three-dimensional computed tomography; SV: splenic vein; SV + P: splenic vein and pancreas; P: pancreas.

## Results

### Dorsal landmarks in 3D-CT and operative videos

The findings of the 3D-CT and the concordance rate between 3D-CT and operative videos are shown in Table 1. Preoperative 3D-CT findings revealed SV type in 12 patients (50%), SV + P type in 7 patients (29%), P type in 1 patient (4%), and unclear type in 4 patients (17%). The concordance rate between preoperative 3D-CT and operative videos was 100% in the SV type (12/12), 57% in the SV + P type (4/7), 0% in the P type (0/1), and 75% in the unclear type (3/4) (Table 1 and Figure 2(a)–(c)). Generally, the concordance rate between 3D-CT and operative videos was 79% (19/24). In this study, crossed cases were found in five patients, of whom three patients were diagnosed with SV + P type, one with P type, and one with unclear type by preoperative 3D-CT simulation (Supplemental Table 1). The four patients in whom we could not predict the dorsal landmark by preoperative 3D-CT included three patients with unclear type and one patient with SV type in the operative videos.

### Patient characteristics and surgical outcomes of the 3D-CT and non-3D-CT groups

There were no differences in clinicopathological characteristics between the 3D-CT and non-3D-CT groups in this study (Table 2).

Table 3 shows the surgical outcomes of the 3D-CT and non-3D-CT groups. The time for dissection of No. 11p LN in the 3D-CT group was significantly shorter than that in the non-3D-CT group (7.7 (3.0–16.2) versus 15.8 (3.9–47.3) min,  $P=0.044$ ). There was no significant difference in the number of retrieved No. 11p LNs (2 (1–5) versus 1 (0–7),  $P=0.124$ ) or total blood loss (0 (0–390) versus 10 (0–200) mL,  $P=0.686$ ) between the 3D-CT and non-3D-CT groups. In the postoperative course, one patient had pneumonia and another patient had cholecystitis in the 3D-CT group, and one patient had atrial fibrillation in the non-3D-CT group. There was no pancreatic fistula or vessel injury in either group.

## Discussion

Using 3D-CT, we could easily predict the dorsal landmark of No. 11p LN. In this study, we used the Ziostation, which is a software that can create 3D-CT images in a short time and at a low cost. We can rotate the created image and diagnose the dorsal landmark in the caudal view, similar to that in the actual view during No. 11p LN dissection in laparoscopic surgery. As a result, we could predict the dorsal landmark of No. 11p LN easier with 3D-CT than with other methods. Moreover, the concordance rate between preoperative 3D-CT and operative videos was extremely high (79%). Thus, we consider 3D-CT to be a simple method with high accuracy for prediction of the dorsal landmark of LN.

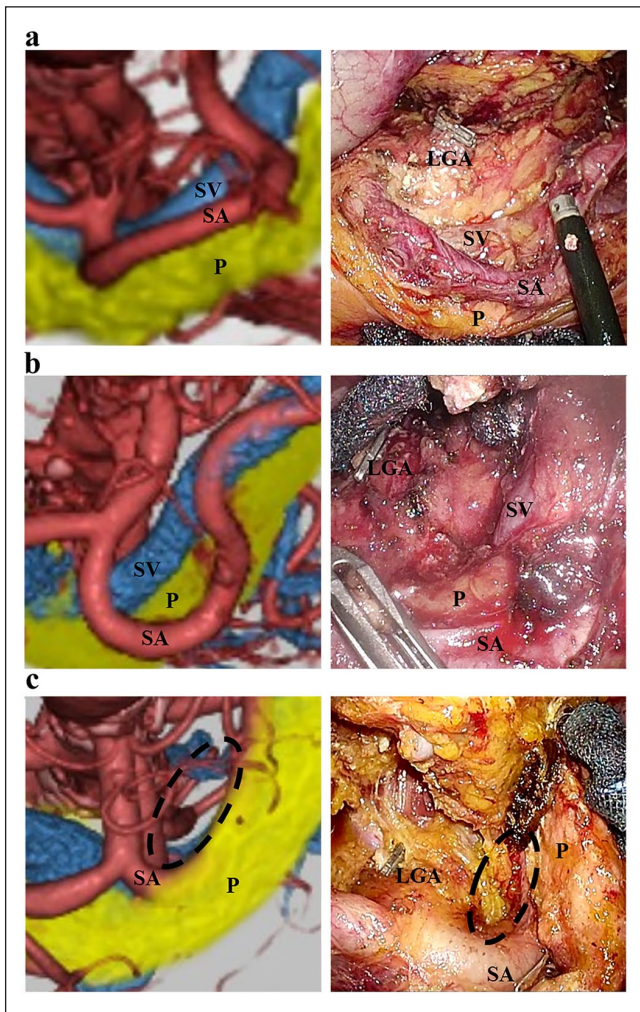


**Figure 2.** Three cases matched the dorsal landmark findings between the 3D-CT and operative video: (a) SV type, (b) SV + P type, and (c) unclear dorsal landmark type. 3D-CT: three-dimensional computed tomography; LGA: left gastric artery; SV: splenic vein; SA: splenic artery; P: pancreas.

This study revealed that the landmark of No. 11p LN dissection was not only the SV or pancreas but also unclear. We could not detect the dorsal landmark of No. 11p LN using preoperative 3D-CT in four patients (17%, 4/24). In the 3D-CT group, the dissection time of the unclear type was longer than that of other types in this study, although the difference was not significant (10.9 (6.5–15.0) versus 7.7 (3.0–16.9) min,  $P=0.55$ ; data not shown). It is well known that the anatomical variation is related to the difficulty in LN dissection in laparoscopic gastrectomy. Zhu et al.<sup>14</sup> reported that the rate of concealed type of splenic artery, where the lowest point of the splenic artery exists at the inferior margin of the pancreas, is 14.2% and that this type has a tendency to longer total operative times and higher morbidity rates. Goto et al.<sup>15</sup> also reported that the depth from the skin to the celiac artery was related to suprapancreatic dissection time. We considered that the dorsal landmark type might be related to the difficulty in No. 11p LN dissection in laparoscopic gastrectomy. Moreover, we could not detect the dorsal landmark during surgery in almost all unclear cases (75%, 3/4). When the dorsal landmark of No. 11p LN was unclear in 3D-CT, we could not likely detect the dorsal landmark during surgery due to the anatomy around the splenic artery. In such cases, discontinuation of No. 11p LN dissection with adequate exposure around the splenic artery is recommended to prevent injury to the vessels and/or pancreas.

Our data showed that the concordance rate of cases where the dorsal landmark was the SV + P or P type by preoperative 3D-CT findings was lower than that of those where the dorsal landmark was the SV type. It is well known that pancreas edges cannot be clearly detected on CT. We considered that this was one of the reasons for the low concordance rate of SV + P or P type. Thus, we should be careful not to injure the pancreas in the SV + P or P type by preoperative 3D-CT findings.

We also revealed that the time of No. 11p LN dissection using 3D-CT was shortened to half of that with conventional CT. Fast detection of the dorsal layer of No. 11p LN allows

**Table 2.** Patient characteristics of the 3D-CT and non-3D-CT groups.

|                                      | 3D-CT group<br><i>n</i> =9 | Non-3D-CT group<br><i>n</i> =23 | <i>P</i> value |
|--------------------------------------|----------------------------|---------------------------------|----------------|
| Age (years)                          |                            |                                 |                |
| Median (range)                       | 78 (63–88)                 | 69 (36–88)                      | 0.172          |
| Sex                                  |                            |                                 |                |
| Male:female                          | 8/1                        | 17/6                            | 0.640          |
| Body mass index (kg/m <sup>2</sup> ) |                            |                                 |                |
| Median (range)                       | 22.2 (16.8–25.3)           | 22.3 (17.0–30.3)                | 0.557          |
| pStage                               |                            |                                 |                |
| Stages I/II, III, IV                 | 4/5                        | 14/9                            | 0.453          |
| Operative method                     |                            |                                 |                |
| LDG/LTG                              | 5/4                        | 8/15                            | 0.426          |
| Dorsal landmark of No. 11p LN        |                            |                                 |                |
| SV/ SV + P/P/unclear                 | 5/1/0/3                    |                                 | –              |

3D-CT: three-dimensional computed tomography; LDG: laparoscopic distal gastrectomy; LTG: laparoscopic total gastrectomy; LN: lymph node; SV: splenic vein; SV + P: splenic vein and pancreas; P: pancreas.

**Table 3.** Surgical outcomes in the 3D-CT and non-3D-CT groups.

|                                       | 3D-CT group    | Non-3D-CT group | P value |
|---------------------------------------|----------------|-----------------|---------|
|                                       | <i>n</i> = 9   | <i>n</i> = 23   |         |
| Total operative time                  |                |                 |         |
| Median (range), min                   | 276 (212–549)  | 275 (214–512)   | 0.629   |
| Total retrieved lymph nodes           |                |                 |         |
| Median (range)                        | 35 (24–54)     | 42 (24–57)      | 0.257   |
| Total metastatic lymph nodes          |                |                 |         |
| Median (range)                        | 3 (0–9)        | 0 (0–21)        | 0.268   |
| Time of No. 11p lymph node dissection |                |                 |         |
| Median (range), min                   | 7.7 (3.0–16.2) | 15.8 (3.9–47.3) | 0.044   |
| Blood loss                            |                |                 |         |
| Median (range), mL                    | 0 (0–390)      | 10 (0–200)      | 0.686   |
| Retrieved lymph nodes of No. 11p      |                |                 |         |
| Median (range)                        | 2 (1–5)        | 1 (0–7)         | 0.124   |
| Metastatic lymph nodes of No. 11p     |                |                 |         |
| Median (range)                        | 0 (0–3)        | 0 (0–2)         | 0.135   |
| Morbidity <sup>a</sup>                |                |                 |         |
| Pancreatic fistula                    | 0              | 0               | –       |
| Vessel injury                         | 0              | 0               | –       |
| Others                                | 2              | 1               | 0.183   |

3D-CT: three-dimensional computed tomography.

<sup>a</sup>Grade II or higher on the Clavien–Dindo classification.

us to perform LN dissection in an easier manner during surgery. Therefore, we considered that preoperative 3D-CT simulation allows the prediction of the dorsal landmark of No. 11p LN and reduces the dissection time. Furthermore, vessel injury and pancreatic fistula did not develop in either group. These rates are lower than those previously reported for D2 LN dissection.<sup>5</sup> Our data suggest that preoperative 3D-CT simulation might allow us to detect the dorsal landmark of LNs smoothly and prevent organ injuries along the splenic artery. Overall, preoperative 3D-CT contributes to a shorter time of No. 11p LN dissection.

There were no significant differences between the total operative time of the 3D-CT and non-3D-CT groups. This may be because many factors, except No. 11p LN dissection, influenced the total operative time in this study. However, we considered that decreasing the dissection time could contribute to operation safety, and preoperative simulation using 3D-CT might be important for clinical practices.

The main limitations of this study are as follows: the sample size in a single institution is small, and the calculation and justification of the sample size have not been selected for this study. We considered that it was important to exclude the effect of learning curve to clarify the efficacy of preoperative 3D-CT simulation. Therefore, we compared cases in which procedures were performed in the short term by one surgeon certified by the Endoscopic Surgical Skill Qualification System in Japan. Thus, the sample size was small in this study. Moreover, two surgeons assessed each image and video recording. Thus, we consider the quality of diagnosis of

the dorsal landmark to be high and that the results regarding dissection time of No. 11p LN are meaningful. Another limitation was that there were more patients who underwent LTG in the non-3D-CT group than in the 3D-CT group. However, the difference in the operative method between both groups was not significant, and the technique of No. 11p LN dissection was common to both LDG and LTG. Therefore, we considered that the difference in the operative method did not influence the surgical outcome of this study.

Therefore, prediction of the dorsal landmark of No. 11p LN using 3D-CT is a simple method with high accuracy that contributes to shortening the time of No. 11p LN dissection in laparoscopic gastrectomy.

### Acknowledgements

The author thanks Noriyoshi Negi (Department of Radiology, Kobe University Hospital, Japan) for his valuable assistance in creating the three-dimensional computed tomography (3D-CT) images.

### Author contributions

T.I. and S.K. contributed to the study concept and design, acquisition of data, statistical analysis, and drafting of the manuscript. T.I., S.K., G.T., N.U., H.H., M.Y., Y.M., K.Y., T.M., T.O., T.N., S.S., and Y.K. helped in the analysis and interpretation of data. Y.K. helped in study supervision. All authors critically revised the manuscript and approved the final version to be published. All authors agreed to be accountable for all aspects of the work in ensuring that questions related to the accuracy or integrity of any part of the work are appropriately investigated and resolved.

## Declaration of conflicting interests

The author(s) declared no potential conflicts of interest with respect to the research, authorship, and/or publication of this article.

## Ethical approval

Ethical approval for this study was obtained from the Institutional Review Board of Kobe University Hospital [170119].

## Funding

The author(s) disclosed receipt of the following financial support for the research, authorship, and/or publication of this article: This work was supported by Japan Society for the Promotion of Science (JSPS) KAKENHI Grant Number JP16K12911.

## Informed consent

Informed consent was obtained from all individual participants included in the study.

## ORCID iD

Taro Ikeda  <https://orcid.org/0000-0002-9202-3482>

## Supplemental material

Supplemental material for this article is available online.

## References

1. Kitano S, Shiraishi N, Uyama I, et al. A multicenter study on oncologic outcome of laparoscopic gastrectomy for early cancer in Japan. *Ann Surg* 2007; 245(1): 68–72.
2. Katai H, Sasako M, Fukuda H, et al. Safety and feasibility of laparoscopy-assisted distal gastrectomy with suprapancreatic nodal dissection for clinical stage I gastric cancer: a multicenter phase II trial (JCOG 0703). *Gastric Cancer* 2010; 13(4): 238–244.
3. Katai H, Mizusawa J, Katayama H, et al. Short-term surgical outcomes from a phase III study of laparoscopy-assisted versus open distal gastrectomy with nodal dissection for clinical stage IA/IB gastric cancer: Japan Clinical Oncology Group Study JCOG0912. *Gastric Cancer* 2017; 20(4): 699–708.
4. Japanese Gastric Cancer Association. Japanese gastric cancer treatment guidelines 2014 (ver. 4). *Gastric Cancer* 2017; 20(1): 1–19.
5. Inaki N, Etoh T, Ohyama T, et al. A multi-institutional, prospective, phase II feasibility study of laparoscopy-assisted distal gastrectomy with D2 lymph node dissection for locally advanced gastric cancer (JLSSG0901). *World J Surg* 2015; 39(11): 2734–2741.
6. Lee SW, Kawai M, Tashiro K, et al. Laparoscopic distal gastrectomy with D2 lymphadenectomy followed by intracorporeal gastroduodenostomy for advanced gastric cancer: technical guide and tips. *Transl Gastroenterol Hepatol* 2017; 2: 84.
7. Kim HI, Hur H, Kim YN, et al. Standardization of D2 lymphadenectomy and surgical quality control (KLASS-02-QC): a prospective, observational, multicenter study [NCT01283893]. *BMC Cancer* 2014; 14: 209.
8. Natsume T, Shuto K, Yanagawa N, et al. The classification of anatomic variations in the perigastric vessels by dual-phase CT to reduce intraoperative bleeding during laparoscopic gastrectomy. *Surg Endosc* 2011; 25(5): 1420–1424.
9. Sunagawa H and Kinoshita T. Three-dimensional computed tomography simulation for laparoscopic lymph node dissection in the treatment of proximal gastric cancer. *Transl Gastroenterol Hepatol* 2017; 2: 54.
10. Wang JB, Huang CM, Zheng CH, et al. Role of 3DCT in laparoscopic total gastrectomy with spleen-preserving splenic lymph node dissection. *World J Gastroenterol* 2014; 20: 4797–4805.
11. Biondi A and Hyung WJ. Seventh edition of TNM classification for gastric cancer. *J Clin Oncol* 2011; 29: 4338–4339.
12. Japanese Gastric Cancer Association. Japanese classification of gastric carcinoma: 3rd English edition. *Gastric Cancer* 2011; 14(2): 101–112.
13. Dindo D, Demartines N and Clavien PA. Classification of surgical complications: a new proposal with evaluation in a cohort of 6336 patients and results of a survey. *Ann Surg* 2004; 240(2): 205–213.
14. Zhu C, Kong SH, Kim TH, et al. The anatomical configuration of the splenic artery influences suprapancreatic lymph node dissection in laparoscopic gastrectomy: analysis using a 3D volume rendering program. *Surg Endosc* 2018; 32(8): 3697–3705.
15. Goto H, Kanaji S, Yasuda T, et al. The depth from the skin to the celiac artery measured using computed tomography is a simple predictive index for longer operation time during laparoscopic distal gastrectomy. *World J Surg* 2018; 42(4): 1065–1072.